WOOD RESEARCH doi.org/10.37763/wr.1336-4561/69.4.647660
e-ISSN 2729-8906
69(4): 2024 647-660 pp.

THE ATTENUATION CHARACTERISTICS OF DIFFERENT FREQUENCY COMPONENTS OF ACOUSTIC EMISSION SIGNAL DURING PROPAGATION IN ELM AND PINE WOOD

KUN DU[1], YOULI WANG[2], ZHIHENG ZHANG[1], MING LI[3,4], SAIYING FANG[1]
[1]SOUTHWEST FORESTRY UNIVERSITY, CHINA
[2]YUNNAN VOCATIONAL INSTITUTE OF ENERGY TECHNOLOGY, CHINA
[3]ANHUI POLYTECHNIC UNIVERSITY,CHINA
[4]KEY LABORATORY OF ADVANCED PERCEPTION AND INTELLIGENT CONTROL OF HIGH-END EQUIPMENT OF MINISTRY OF EDUCATION, CHINA

(RECEIVED NOVEMBER 2024)

ABSTRACT

In order to gain a deeper understanding of the attenuation characteristics of different frequency components of acoustic emission signal when propagating in wood, this research conduct pencil lead fracture experiments on the surface of elm and pine specimen. Original AE signals acquired by different sensors are decomposed using 5-level wavelet transform, the attenuation characteristics of different frequency components are studied, and the acoustic emission source is located according to the energy of different frequency components. The results indicate that the propagation distance is the main factor affecting the attenuation of AE signals. The longer the propagation distance, the greater the degree of attenuation. The attenuation characteristics of high-frequency components of acoustic emission signals deviate from the ideal attenuation model after the propagation distance greater than 10 cm. The higher the frequency components of acoustic emission signals, the faster they attenuatewhen propagation in elm and pine specimen.

KEYWORDS:Acoustic emission, frequency components, attenuation characteristics, wood.

INTRODUCTION

Acoustic emission (AE) is a phenomenon in which local sources in materials rapidly release energy to generate transient elastic waves. When material or structure is subjected to stress, the unevenness of its microstructure and the presence of defects lead to local stress concentration, resulting in unstable stress distribution. AEtechnologyas a non-destructive

testing method, has been widely used in fields such as wood science(Shen et al. 2015a,b, Liet al. 2020, Ding et al. 2021, Xu et al. 2023a,b Qin et al. 2024), structural health monitoring(Bakuckas et al. 1994, Zhao et al. 2000, Vun et al. 2005), and non-destructive evaluation of materials(Zhao et al. 2000, Satour et al. 2013, Shen et al. 2015a, Zhao et al. 2022, Du et al. 2024). It achieves real-time monitoring of the internal state of materials by capturing the elastic waves generated by stress changes or damage inside materials.

AE technology provides an effective means for evaluating the mechanical properties of wood, detecting internal defects, and understanding the microscopic behavior of wood under stress.Many scholars have extensively explored the propagation characteristics of AE signals in wood. These studies reveal the intrinsic relationship between the acoustic properties of wood and its physical and mechanical properties, providing a foundation for understanding the propagation of AE signals in wood. Li et al.(2021) used wavelet analysis to decompose and reconstruct AE signals, and calculated the propagation speed of AE signals in pine specimen using the reconstructed AE signals, determining the effective frequency bands for AE signals propagation on surface and inside of pine. Ju et al.(2018) used wavelet analysis to analyze the AE signals on the surface of horsetail glued laminated wood, and found that there were significant differences in the propagation speed in both the longitudinal and transverse directions. In addition, changes in wood structure, propagation characteristics, and air medium had significant impact on AE signals. Wang et al.(2021)generated simulated AE sources in pine and beech specimens using fracture lead cores and thin wood strips, and studied the propagation speed of different AE signals using wavelet analysis and correlation analysis. Their results indicate that using signals generated by fracture thin wood strips to research the propagation speed of AE signals in wood can obtain more objective results.Li et al.(2020) showed that changes in wood moisture content significantly affect the propagation speed and energy of AE signals.Shen et al.(2015) proposed a method for locating AE source based on the principle of triangular geometric localizationusing time difference method. The results indicate that this method can accurately identify the specific location of AE source. Li et al.(2021) showed that the propagation speed of AE signal transverse and longitudinal wave was greatly influenced by medium, and longitudinal wave mainly propagate along the cell wall of wood fiber cells. Ding et al.(2021)used singular spectrum analysis (SSA) to denoise original AE signals and then used correlation analysis to calculate the propagation speed, thus the accuracy of AE source linear localization algorithm can be significantly improved.

However, the propagation process of AE signals in complex porous medium such as wood, especially the attenuation characteristics of different frequency components, is still an issue that is not fully understood. The complex structure of wood, including its anisotropy, non-uniformity, and naturally occurring defects greatly affects the propagation and attenuation of AE signals.Further in-depth research is needed on the attenuation characteristics of different frequency components of AE signals in wood and their quantitative relationship with wood structural characteristics.This research selects the Daubechies (db10) wavelet basis function with high vanishing moment and good regularity to decompose original AE signals. Due to the sampling frequency being set to 500 kHz, after 5-level wavelet decomposition, the high-frequency detail signal bands are 125–250, 62.5–125, 31.25–62.5, 15.625–31.25, and 7.8125-15.625 kHz, respectively, which cover all possible frequency range of these AE

signals.

AE signal can be considered as AC current, and the heat generated when AE signal through a 1Ω resistor is taken as energy.Since these signals acquired by AE sensors are discontinuous AE signals with $1/f_s$ seconds between two data, assuming that the discretization process uses a zero-order retainer, that is to say, the amplitude of AE signal remains constant during this period, so the energy of AE signal is calculated as(Liet al. 2021, Ding et al. 2022, Fang et al. 2022):

$$E=\sum_{i=1}^{n}\Delta t_i\cdot u_i^2=T\sum_{i=1}^{n}u_i^2,\Delta t_i=T=1/\ f_s,i=1,2...n \qquad (1)$$

where: n is the data length and $f_s$is the sampling frequency. The location of the AE source is obtainedas follow (Zhu 2011, Du et al. 2024):

$$x=\frac{(x_1+x_3)\ln(E_6/E_1)-(x_1+x_6)\ln(E_3/E_1)}{2\ln(E_6/E_1)-2\ln(E_3/E_1)} \qquad (2)$$

where:x_1, x_3, and x_6 are the position coordinates of sensors S_1, S_3, and S_6, and E_1, E_3, E_6 are the energy of different frequency components of AE signals acquired by S_1, S_3, and S_6, resp.

This research aims to explore in depth the attenuation characteristics of various frequency components of AE signals during propagation in wood. By analyzing these frequency dependent attenuation laws, we expect to establish a more accurate AE signal propagation model, providing theoretical basis and technical support for wood quality assessment, structural health monitoring, and optimization of wood processing processes.

MATERIALS AND METHODS

The experimental setup is shown in Fig. 1. Dried elm and pine specimens with straight grain are sawn into dimensions of 800 mm (axial) × 100 mm (tangential) × 20 mm (radial).The density and moisture content of the elmspecimen are 680±5 kg/m^3 and 10.4±0.5%,and the pine specimen are 422±5 kg/m^{3}11.8±0.5%, resp. The methods for determining wood density and moisture contentareaccording toGB/T 1933-2009 and GB/T 1931-2009.

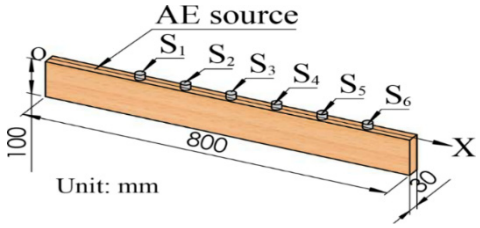

Fig. 1: Schematic presentation of the experimental setup.

Six single resonant AE sensors(Beijing Soundwel Technology Co., Ltd., Beijing, China) are fixed on the upper surface of wood specimens, their position coordinates are 200, 300, 400

500, 600, 700mm. A six-channels high-speed data acquisition system is constructedutilizing LabVIEW software (National Instruments) and NIUSB-6366 high-speed acquisition card (National Instruments). The gain of this preamplifier (Beijing Soundwel Technology Co., Ltd., Beijing, China) is 40 dB, and the output voltage of this amplifier is −10 to 10 V. Because the frequency range of AE signals propagating in wood is mainly distributed in 0–200 kHz(Bakuckas et al. 1994, Vun et al. 2005, Shen et al. 2015a, Ju et al. 2018, Li et al. 2020a, Li, et al. 2021a,b Wang et al. 2021, Xu et al. 2023, Du et al. 2024), according to Shannon's sampling theorem, to recover actual AE signals from original signals without distortion, the sampling frequency f_s should be twice the maximum frequency f_{max} of original signals or higher (i.e. $f_s \geq 2f_{max}$). Therefore, the sampling frequency is set to 500 kHz in this research.

In this research the lead core is fractured to simulate burst AE signals indicating wood damage. To make the AE signals as consistent as possible, the lead core fractureexperiments are conducted in accordance with the ASTM E976-2015"Standard guide for determining the reproducibility of AE sensor response". These AE signals are generated by fracture lead core with a length of 2.5 mm and a diameter of 0.5 mm at an angle of 30°. Vacuum-insulating grease is applied between specimens and these AE sensors to assure sufficient coupling, thus reducing influence of air on results.

RESULTS

Figs. 2 and 3 is the waveform and spectrum of six original AE signals acquired by (a, b)S_1, (c, d)S_2, (e, f)S_3, (g, h)S_4, (i, j)S_5, and (k, l)S_6 when lead core is fracturedat the locationx_1=100 mm on the upper surface of elmand pinespecimen.Fracture lead core generates burst AE signals with short duration, so only the AE signals with duration of 8msare captured and analyzed. From the time-domain waveforms on the left side of Figs. 2 and 3, one can roughly observe the attenuation of these signals and the changes in high-frequency and low-frequency components.These AE signals have large amplitude in early stage but significant decrease in later stage, indicating that the amplitude of AE signals rapidly decreasein spatiotemporal. The AE signals acquired by sensors S_1, S_2, and S_3 have dense waveform in early stage, and it can be considered that these AE signals in this stage are mainly composed of high-frequency components. However, these AE signals acquired by sensors S_4, S_5, and S_6 become sparser in early stage, indicating significant attenuation in high-frequency components.The peak frequency of original signals shown in the right sideis less than 8 kHz, which is lower than frequency response bandwidth of these AE sensors. This is mainly because the AE signalsare generated instantaneously when the lead core is fractured,the energy of these AE signals is weak and the duration is short, thus noise accounted for a large proportion of original AE signals(Wang et al. 2021, Xu et al. 2023). Therefore, it is necessary to process original AE signals to obtain more realistic AE signals.

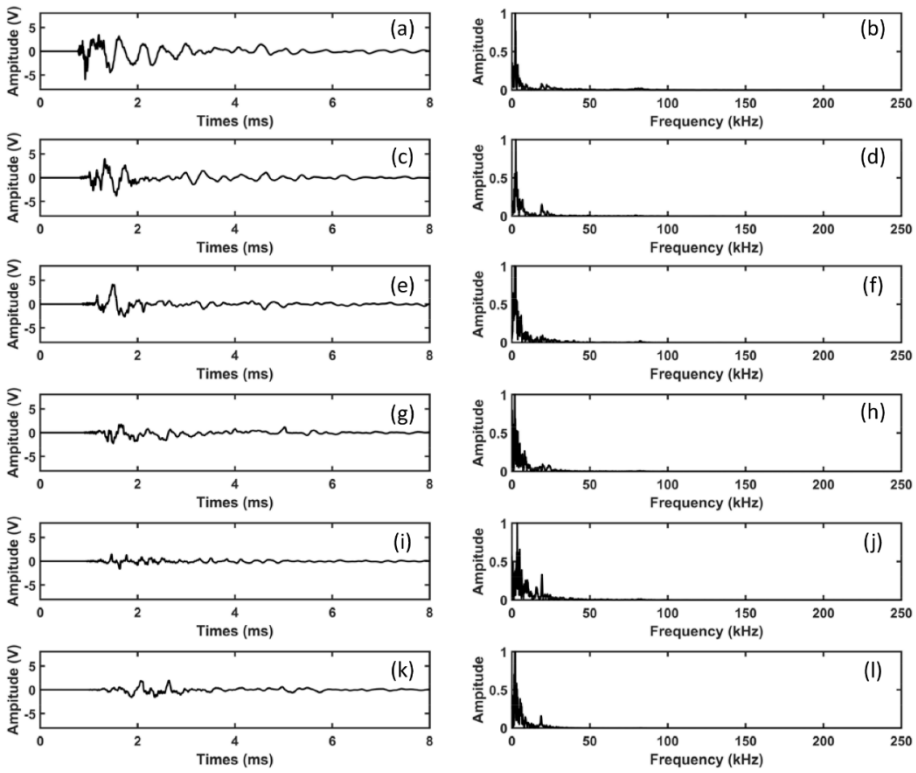

Fig. 2: Waveform and spectrum of six original signals acquired by (a, b)S_1, (c, d)S_2, (e, f)S_3, (g, h)S_4, (i, j)S_5, and (k, l)S_6on elm specimen, resp.

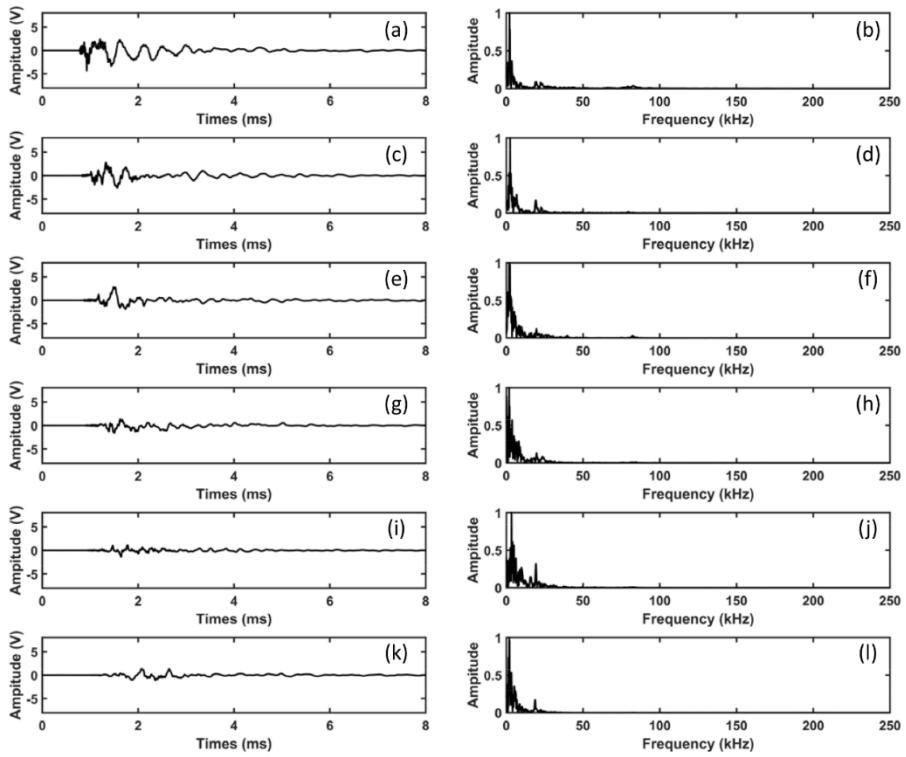

Fig. 3: Waveform and spectrum of six original signals acquired by (a, b)S_1, (c, d)S_2, (e, f)S_3, (g, h)S_4, (i, j)S_5, and (k, l)S_6on pine specimen, resp.

The original signals acquired by S_1 when lead core is fractured at the location x_1=100 mmon the surface of elmand pine specimen are performed 5-level wavelet decomposition, and the detail signals of each level in time-domain and frequency-domain are shown from top to bottom in Figs. 4 and 5.The frequency of the first level detail signal is approximately 165 kHz, and the waveform exhibit small amplitude and short duration.The frequency of the fifth level detail signal is approximately 7 kHz, which is less than frequency response bandwidth of the AE sensor. Therefore, the fifth level detail signalis considered as low-frequency noise signal. Hence, the first, second, third, and fourth level detail signalsare selected for reconstruction.Fracture lead core on wood surface will generateAE signals of different frequency components. Due to factors such as wood viscosity and internal porous structure, some frequency components will be filtered out when propagating in wood. As shown in Figs. 4 and 5, it can be seen that the distribution difference of frequency components of AE signals is relatively small when propagating inelm and pine specimens.

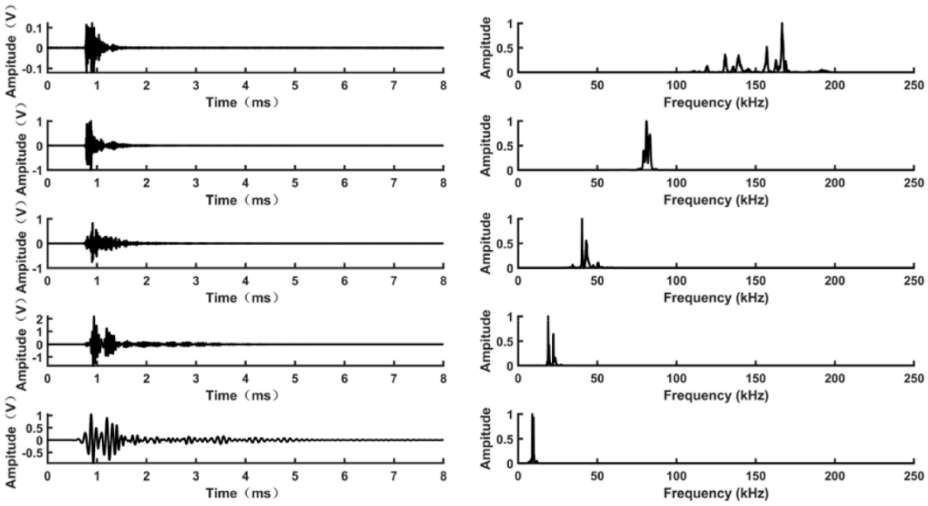

Fig. 4: Waveforms and spectra of detail signals at each level of the original signal acquired by S_1on elm specimen.

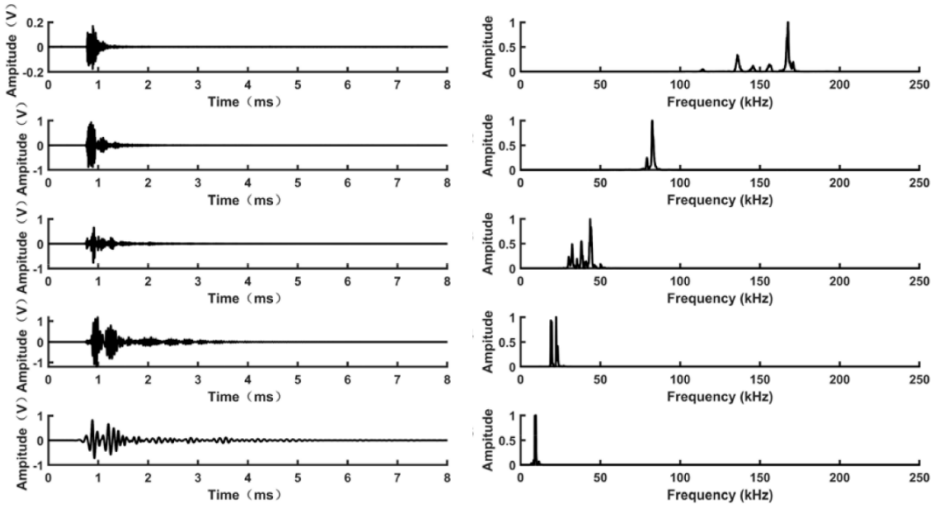

Fig. 5: Waveforms and spectra of the detail wavelet decomposition signals at each level of the original signal acquired by S_1 on pine specimen.

Attenuation characteristics of different frequency components

In order to research the attenuation characteristics of AE signals at different frequency components during propagation in elm and pine specimens, perform 5-level wavelet decomposition on original AE signals generated by fracture lead core at the location x_1=100 mm, then the energy of the first, second, third, and fourth level detail signals is calculated according to Eq.1. The propagation distance between the AE source and the AE sensors is considered as independent variable, and an exponential function is used to fit the relationship between the energy of different detail signals and propagation distance.In order to reduce experimental errors caused by random factors, 10 independent experiments are conducted under same conditions, and the average results of the 10 experiments are shown in Figs.6 and 7. When AE signals propagate in elmspecimen, the relationship between the energy of the first, second, third, and fourth level detail signals and the propagation distance is shown in Fig.7.The fitting functions are as follows: $E_1 = 14.37e^{-30.54x}$, $E_2 = 551.93e^{-24.93x}$, $E_3 = 77.31e^{-10.02x}$, $E_4 = 438.50e^{-5.17x}$,and thefitting degrees of these functions are: $R_1^2 = 0.999$, $R_2^2 = 0.998$, $R_3^2 = 0.990$, $R_4^2 = 0.994$, resp. When AE signals propagate in pine specimen, the relationship between the energy of the first, second, third, and fourth level detail signals and the propagation distance is shown in Fig.7. The fitting functions are as follows: $E_1 = 29.69e^{-33.15x}$, $E_2 = 800.51e^{-28.97x}$, $E_3 = 47.26e^{-10.08x}$, $E_4 = 242.49e^{-5.17x}$, and thefitting degrees of these functions are: $R_1^2 = 0.999$, $R_2^2 = 0.997$, $R_3^2 = 0.996$, $R_4^2 = 0.993$, resp.The results indicate that the fitting function can reflect energy attenuation characteristics of different detail signals. Signals in different levels have obvious energy attenuation characteristics, but there are significant differences in attenuation rate.

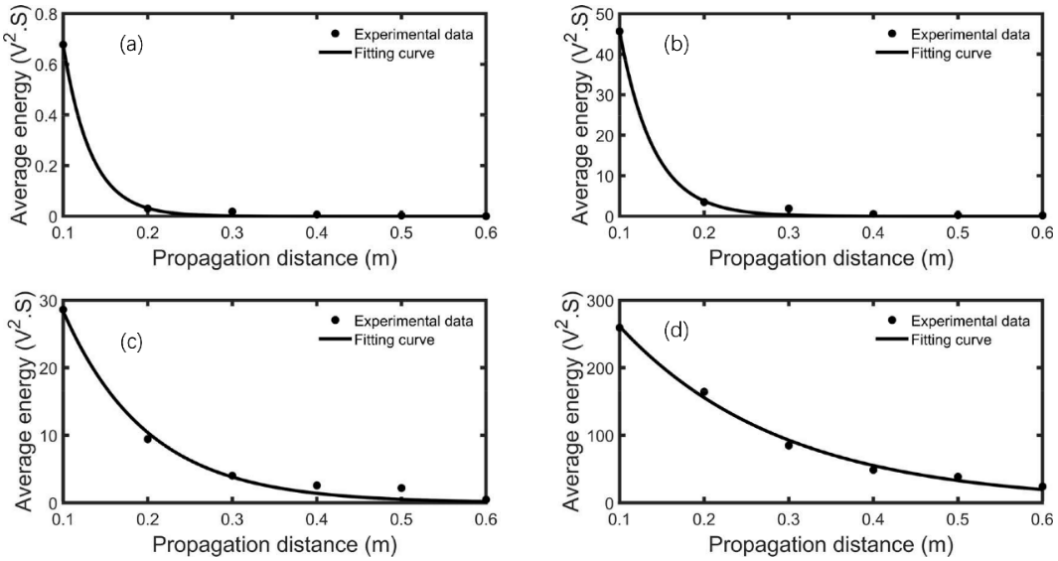

Fig.6: The energy of the (a)first, (b)second, (c)third, (d)fourth level detail signal when AE signals propagate inelm specimen.

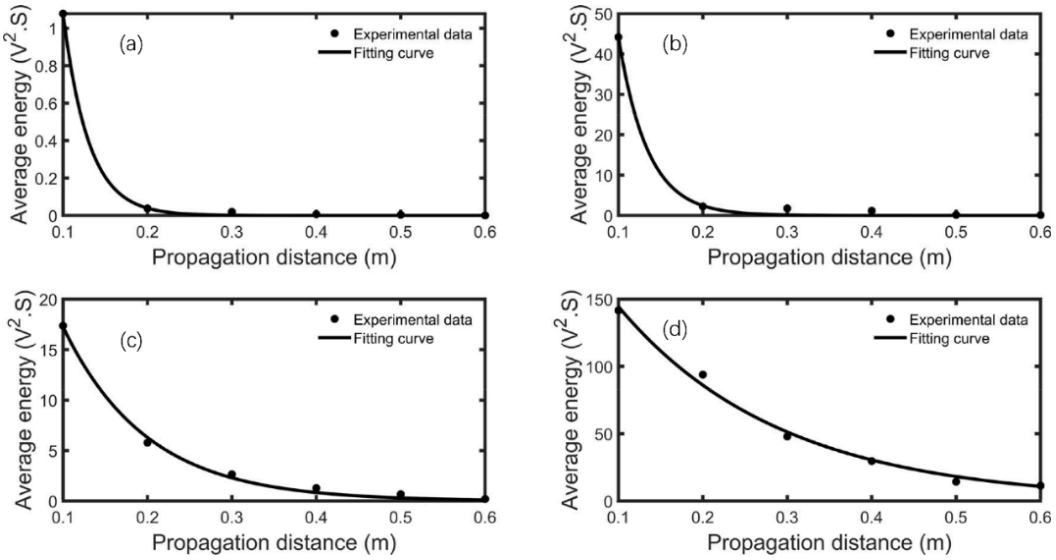

Fig.7: The energy of the (a)first, (b)second, (c)third, (d)fourth level detail signal when AE signals propagate inpine specimen.

AE source localization based on attenuation characteristics of different frequency components

By using the Eqs.1 and 2, it is possible to perform line localization of AE source on wooden specimen without measuring the speed of AE signal and the time it reachesAE sensor. The original AE signals acquired by S_1, S_3 and $S_6$when lead coresare fractured at the location x_2=350 mmarepreformed 5-level wavelet decomposition.The energy of the first, second, third, and fourth level detail signals is calculated according to Eq. 1. In order to reduce experimental errors caused by random factors, 10 independent experiments are conducted under same conditions, and the localization results are listed in Tabs. 1 and 2. Tab. 1 shown the coordinates of AE source obtained in accordance with Eq. 2 based on the energy of different level detail signals when AE signals propagation in elmspecimen. When using the energy of the first to fourth level detail signals for AE source localization, the average localization errors are 12.4, 10.7, 7.8, and 4.2 mm, respectively. However, when using the energy of the original AE signals for localization using same method, the average localization error is 19.2mm. Tab. 2 shown the coordinates of AE source obtained in accordance with Eq. 2 based on the energy of different level detail signals when AE signals propagation in pine specimen. When using the energy of the first to fourth level detail signals for AE source localization, the average localization errors are 13, 11.2, 10, and 4.4 mm, respectively. However, when using the energy of the original AE signals for localization using same method, the average localization error is 21.3 mm.Note that in Tabs. 1 and 2, $x\text{-}_i$ (i=1,2,3,4) represents the coordinate values are calculated based on the energyof i-th level detail signals and Eq. 2, while $x\text{-}_O$ represents the coordinate values are calculated based on the energy of original signals and Eq. 2. The AE source localization results indicate that due to the significant attenuation of high-frequency components of AE signals during propagation, there are significant errors in using the energy of high-frequency components or original signals for localization. On the contrary, the accuracy of locationing using the energy of low-frequency components is significantly improved.

Tab. 1: Localization results of 10 independent experiments using the energy of different detail signalswhen lead coresare fractured at the locationx_2=350 mmon elm specimen.

Serial number	Location coordinates (mm)				
	x_1	x_2	x_3	x_4	x_0
1	364	362	358	354	335
2	363	361	356	356	327
3	362	363	340	353	334
4	338	339	358	346	369
5	336	341	359	345	372
6	339	343	357	346	328
7	340	361	342	354	333
8	362	362	343	355	370
9	363	361	357	353	367
10	337	340	342	346	329

Tab.2: Localization results of 10 independent experiments using the energy of different detail signals when lead coresare fractured at the locationx_2=350 mm on pine specimen.

Serial number	Location coordinates (mm)				
	x_1	x_2	x_3	x_4	x_0
1	363	363	357	353	373
2	365	362	358	354	332
3	364	339	343	356	371
4	361	340	344	353	372
5	337	338	357	346	332
6	335	342	359	347	331
7	338	361	342	354	374
8	362	360	343	355	371
9	363	363	344	345	327
10	338	362	359	343	374

DISCUSSION

There is no absolute answer to the question of whether AE signals attenuate faster in coniferous wood or broad-leaved wood, as it depends on the combined effects of multiple factors. Broad-leaved wood usually has high density and has evolved tubular pore structure, resulting in relatively fast water transport speed. The fiber arrangement of broad-leaved wood may not be as neat as coniferous wood, and it usually contains more pores and cracks. Coniferous wood usually has lower density, smaller tracheid diameter, and slower water transport speed. The fibers of coniferous wood are arranged neatly and the texture is straight, which may have a certain impact on the propagation and attenuation characteristics of AE signals. Due to the presence of numerous pores and cracks in broad-leaved wood, these defects may become scattering sources for AE signals, making high-frequency signals more susceptible to scattering and absorption in broad-leaved wood, resulting in faster attenuation. However, although coniferous wood has neatly arranged fibers, its smaller density and tubular diameter may also cause certain obstacles to signal propagation. On the other hand, the moisture content of wood has a significant impact on the attenuation of AE signals(Liet al.

2020a,b, He et al. 2024). Generally speaking, wood with higher moisture content has stronger scattering and absorption effects on AE signals. Therefore, if there is a difference in moisture content between coniferous wood and broad-leaved wood, this difference may also affect the attenuation characteristics of AE signals in both types of wood.

The phenomenon of rapid attenuation of high-frequency components and slow attenuation of low-frequency components in AE signals when propagating in wood may be influenced by multiple factors. The following attempts to explain the reasons for this phenomenon from three aspects: physical mechanism, material properties, and signal characteristics.

In terms of physical mechanism, AE signals diffuse and propagate from the AE source in all directions. As the propagation distance increases, the area covered by the wavefront continues to expand, and the energy of the AEsignal also continuously diffuses, resulting in a gradual decrease in the energy per unit area and a gradual decrease in the amplitude of the wave(Noguchi et al. 1985, Bakuckas et al. 1994, Aicher et al. 2001). High-frequency signals, due to their short wavelength, are more likely to disperse energy during diffusion, resulting in faster attenuation. In addition, due to the viscoelasticity of wood, there is internal friction between particles, which converts a portion of the mechanical energy ofAE signals into internal energy and absorbs it by the material(Gong et al. 2006, Campbell et al. 2018, Ding et al. 2022, Fang et al. 2022). The energy of the AE signals decreases and the amplitude gradually decreases. This form of attenuation is greatly affected by the viscoelasticity of material and is proportional to frequency of the wave. High-frequency signals experience faster energy loss and more significant attenuation due to their faster vibration speed and more frequent friction with the interior of the wood. Finally, defects such as pores, cracks, and knots in wood can become scattering sources for AE signals. High-frequency signals are more susceptible to the influence of these scattering sources due to their short wavelength, resulting in irregular reflections and reducing the energy of AE signals in their original propagation direction(Zhao et al. 2022, Xu et al. 2023a,b, Qin et al. 2024).

In terms of material properties, wood is porous material with uneven internal structure, and its cells, gaps, and pores form different types of micro pores. These holes hinder the propagation of AE signals, especially for high-frequency signals. In addition, moisture content can affect the density and pore structure of wood, thereby affecting the propagation and attenuation of AE signals in wood. Generally speaking, the higher the moisture content, the stronger the absorption and scattering of AE signals by wood, and the faster the attenuation of high-frequency signals.

In terms of signal characteristics, the degree of attenuation of AE signals is closely related to their frequency(Li et al. 2018, Qin et al. 2022). High-frequency signals are more susceptible to scattering and absorption during propagation due to their short wavelength and concentrated energy, resulting in faster attenuation. Low-frequency signals, due to their longer wavelength and dispersed energy, experience relatively less obstruction during propagation, resulting in slower attenuation.

CONCLUSIONS

The research results indicate that the propagation distance is the main factor affecting the attenuation of AE signals. The longer the propagation distance, the greater the degree of attenuation and the lower signal-to-noise ratio. Secondly, the attenuation characteristics of high-frequency components of AE signals deviate from the ideal attenuation model after the propagation distance greater than 10 centimeters.Thirdly, the higher the frequency components, the faster they attenuate when propagation in elm and pine specimen.

There are still some shortcomings in this research. Firstly, the research may not have fully considered the impact of wood diversity on the attenuation characteristics of AE signals, which limits the generalizability of experimental results. Secondly, there is a lack of in-depth exploration of the attenuation mechanisms of different frequency components. It should be emphasized that the above shortcomings or deficiencies are hypothetical views based on general research paper evaluation criteria and relevant knowledge in the field. To accurately evaluate the specific shortcomings or deficiencies of this research, it is necessary to read the content of this paper in detail and conduct in-depth analysis. Although this research has application value in AE detection, its shortcomings or deficiencies still need to be fully considered.

ACKNOWLEDGEMENTS

The authors express their sincere appreciation for the backing of the National Natural Science Foundation of China (32160345, 31760182), Startup fund for introducing talents and scientific research of Anhui University of Engineering (2021YQQ037), the Teaching Science Research Project (YB202413), and Yunnan Provincial Agricultural Joint Special Program (202401BD070001-121).

REFERENCES

1. Aicher, S., L. Hofflin, and G. Dill-Langer. (2001). Damage evolution and acoustic emission of wood at tension perpendicular to fiber. *Holz als Roh-und Werkstoff*, *59*(1-2), 104-116.
2. Bakuckas, J. G., W. H. Prosser, and W. S. Johnsont. (1994). Monitoring damage growth in titanium matrix composites using acoustic emission. *Journal of Composite Materials*, *28*(4), 305-328.
3. Campbell, L., K. Edwards, R. Lemaster, et al. (2018). The use of acoustic emission to detect fines for wood-based composites, Part one: Experimental setup for use on particleboard. *Bioresources*, *13*(4), 8738-8750.
4. Ding, R., S. Fang, R. Luo, et al. (2022). Propagation characteristics and energy attenuation law of surface shear waves and internal longitudinal waves in Mongolian scotch pine sawn timber based on acoustic emission. *Chinese Journal of Wood Science and Technology*, *36*(01), 36-42.

5. Ding, R., R. Luo, F. Lai, et al. (2021). Straight line location algorithm of wood acoustic emission source based on singular spectrum analysis and signal correlation analysis methods. *Journal of Northwest Forestry University*, *36*(5), 173-178+245.
6. Du, K., M. Li, S. Fang, et al. (2024). Determine the location of acoustic emission source on wood surface by using a wavelet-energy attenuation method. *Wood Material Science & Engineering*.
7. Fang, S., M. Li, T. Deng, et al. (2022). Study on the time-frequency characteristics and propagation law of acoustic emission longitudinal waves in wood grain direction.
8. Gong, B., H. Qi, C. Ma, et al. (2006). A new method of energy location for acoustic emission source. *Technical Acoustics*, *25*(2), 107-109.
9. He, J., Y. She, and M. Li. (2024). Characteristics of acoustic emission parameters of cedar wood damage with different moisture contents. *Journal of Northeast Forestry University*, *52*(2), 91-105.
10. Ju, S., X. Li, T. Luo, et al. (2018). Characteristics of acoustic emission signals on the surface of masson pine gulam with wavelet analysis method. *Journal of Northeast Forestry University*, *46*(08), 84-90.
11. Li, M., M. Wang, R. Ding, et al. (2021a). Study of acoustic emission propagation characteristics and energy attenuation of surface transverse wave and internal longitudinal wave of wood. *Wood science and technology*, *55*(6), 1619-1637.
12. Li, X., T. Deng, and M. Wang. (2021b). Frequency domain identification of acoustic emission signals on surfaceand interior of *Pinus sylvestris* var.mongolica based on wavelet analysis. *Journal of Northwest Forestry University*, *36*(04), 209-213+288.
13. Li, X., T. Deng, M. Wang, et al. (2020a). Linear positioning algorithm improvement of wood acoustic emission source based on wavelet and signal correlation analysis methods. *Journal of Forestry Engineering*, *5*(3), 138-143.
14. Li, X., S. Ju, T. Luo, et al. (2020b). Effect of moisture content on propagation characteristics of acoustic emission signal of *Pinus massoniana* Lamb. *European Journal of Wood and Wood Products*, *78*(1), 185-191.
15. Li, X., M. Li, and S. Ju. (2020c). Frequency domain identification of acoustic emission events of wood fracture and variable moisture content. *Forest Products Journal*, *70*(1), 107-114.
16. Li, Y., S. Yu, L. Dai, et al. (2018). Acoustic emission signal source localization on plywood surface with cross-correlation method. *Journal of Wood Science*, *64*(2), 78-84.
17. Noguchi, M., S. Okumura, and S. Kawamoto. (1985). Characteristics of acoustic emissions during wood drying. *Journal of the Japan Wood Research Society*, *31*(3), 171-175.
18. Qin, G., M. Li, S. Fang, et al. (2022). Study on the dispersion characteristics of wood acoustic emission signal based on wavelet decomposition. *Wood Research*, *67*(6), 966-978.
19. Qin, G., M. Li, S. Fang, et al. (2024). Study of a grid-based regional localization method for damage sources during three-point bending tests of wood. *Construction and Building Materials*, *419*.

20. Satour, A., S. Montrésor, M. Bentahar, et al. (2013). Acoustic emission signal denoising to improve damage analysis in glass fibre-reinforced composites. *Nondestructive Testing And Evaluation*, *29*(1), 65-79.
21. Shen, K., X. Ding, H. Zhao, et al. (2015a). Acoustic emission signal source localization in wood surface with triangle positioning method. *Journal of Northeast Forestry University*, *43*(04), 77-81+112.
22. Shen, K., H. Zhao, X. Ding, et al. (2015b). Acoustic emission signal wavelet disjunction in wood damage fracture process. *Journal of Henan University of Science and Technology: Natural Science*, *36*(3), 33-37.
23. Vun, R. Y., C. dehoop, and F. C. Beall. (2005). Monitoring critical defects of creep rupture in oriented strandboard using acoustic emission: incorporation of EN300 standard. *Wood science and technology*, *39*(3), 199-214.
24. Wang, M., T. Deng, S. Fang, et al. (2021). Generation and characteristics of simulated acoustic emission source of wood. *Journal of Northeast Forestry University*, *49*(06), 96-101+118.
25. Xu, N., M. Li, S. Fang, et al. (2023a). Research on the detection of the hole in wood based on acoustic emission frequency sweeping. *Construction and Building Materials*, *400*, 132761.
26. Xu, N., M. Li, S. Fang, et al. (2023b). Study the effects of ferrous materials inside wood on the propagation characteristics of acoustic emission signals. *Wood Material Science & Engineering*, *18*(5), 1650-1662.
27. Zhao, F., J. Luo, C. Tian, et al. (2000). The crack growth process of particulate filled polymer monitored by acoustic emission. *Chinese Journal of High Pressure Physics*, *12*(03), 235-240.
28. Zhao, Y., M. Li, S. Fang, et al. (2022). Influence of boundary conditions on acoustic emission propagation characteristics of Zelkova schneideriana. *Journal of Wood Science*, *68*(1), 62.
29. Zhu, X. (2011). New location method for acoustic emission source by energy. *China Measurement & Test*, *37*(1), 18-20.

KUN DU, ZHIHENG ZHANG, SAIYING FANG
SOUTHWEST FORESTRY UNIVERSITY
BAILONG ROAD 300, PANLONG DISTRICT, KUNMING
CHINA

YOULI WANG
YUNNAN VOCATIONAL INSTITUTE OF ENERGY TECHNOLOGY
WENYUAN NORTH ROAD, VOCATIONAL EDUCATION PARK, QUJING
CHINA

MING LI*
[1] ANHUI POLYTECHNIC UNIVERSITY, BEIJING MIDDLE ROAD, WUHU, CHINA
[2]KEY LABORATORY OF ADVANCED PERCEPTION AND INTELLIGENT CONTROL OF HIGH-END EQUIPMENT OF MINISTRY OF EDUCATION
CHINA
*Corresponding author: 1841719811@qq.com